Sustainable Materials and Technologies 36 (2023) e00591

Contents lists available at ScienceDirect

Sustainable Materials and Technologies

journal homepage: www.elsevier.com/locate/susmat

Effects of mechanical cell disruption on the morphology and properties of spirulina-PLA biocomposites

Kuotian Liao [a], Paul Grandgeorge [a], Andrew M. Jimenez [a], Bichlien H. Nguyen [b,c], Eleftheria Roumeli [a,*]

[a] Department of Materials Science and Engineering, University of Washington, Seattle, WA, USA
[b] Microsoft Research, Redmond, WA, USA
[c] Paul G. Allen School of Computer Science and Engineering, University of Washington, Seattle, WA, USA

ARTICLE INFO

Keywords:
Biocomposites
Spirulina
Polylactic acid
Probe sonication
Mechanical properties
Global warming potential

ABSTRACT

Biocomposite materials offer a promising strategy to satisfy the increasing demand for sustainable plastics. While the incorporation of biopolymers extracted from plants and microorganisms (e.g., cellulose) as fillers in various polymer matrices has demonstrated encouraging properties, biopolymer extraction often requires wasteful mechanical and chemical treatments, thus limiting the overall environmental benefits. As alternative, an emerging approach makes use of fillers made up of less-refined biological material (biomatter) which retains the original chemical composition and hierarchical structure of the source organism, hence bypassing the energy intensive extraction steps. Here, we introduce a novel set of biocomposite materials obtained by compounding polylactic acid (PLA), one of the most consumed industrially degradable plastics, with spirulina, an abundant and fast-growing microalgal species serving as a filler. Specifically, we study the effect of using spirulina in a raw or physically dissociated form after Sonication. We find that independently of the filler pretreatment, the Young's modulus remains as high as neat PLA, while the elongation to break, strength, and toughness progressively decrease with increasing spirulina content. We show that the use of dissociated spirulina enhances the tensile strength by up to 25% compared to biocomposites made with unprocessed spirulina, as a result of the improved filler dispersion and reduced particle size. Our findings also reveal drastically enhanced moisture-induced plasticization in the biocomposites with dissociated spirulina. We report a remarkable 90% toughness increase with mechanically pretreated spirulina at a concentration of 9.1 wt% when compared to the non-water plasticized biocomposite at the same filler concentration, even rivaling the toughness of neat PLA. Finally, we provide estimates for the reduced global warming potential of the produced biocomposites, as compared to neat PLA. Our study presents a holistic view of the performance of PLA-spirulina biocomposites and demonstrates the effectiveness of physical filler dissociation as a means to improve the strength and toughness of the biocomposites.

1. Introduction

Since the start of their large-scale proliferation in the 1950s, plastics have become an integral part of our society. Today, the accumulation of plastic waste in the biosphere (often resulting from improper disposal) is posing serious environmental and ecological challenges that will likely lead to catastrophic and irreversible consequences [1]. Over the past decades, research efforts to mitigate plastic pollution by developing biodegradable and renewable alternatives to traditional petroleum-derived plastics have gathered unprecedented levels of interest [2].

For example, polylactic acid (PLA) has emerged as one of the most promising bio-based and biodegradable polymers. The possibility to tightly control the molecular composition of end products, combined with its excellent processability as well as the relatively low cost and abundance of its feedstock, has given PLA significant advantages over other bio-based polymers such as starch blends or polyhydroxyalkanoates (PHA) [3–8]. Numerous literature reports focusing on compounding PLA with other polymers or fillers demonstrate avenues to control specific properties of the resulting composites, such as strength and toughness [9–13].

Biocomposites offer a promising strategy to further mitigate the detrimental environmental impact of polymers. In the case of

* Corresponding author.
E-mail address: eroumeli@uw.edu (E. Roumeli).

https://doi.org/10.1016/j.susmat.2023.e00591
Received 27 December 2022; Received in revised form 3 February 2023; Accepted 19 February 2023
Available online 22 February 2023

biocomposites, extracted biopolymers, such as cellulose, chitin, starch or protein are incorporated as fillers into a polymer matrix. However, the energy- and resource-intensive extraction and purification process to obtain such biopolymers from raw biomass can be limiting factors to the environmental (and financial) advantages of their biocomposites [14].

An alternative approach is blending polymer matrices with biological materials (biomatter) in minimally processed states, i.e., as entire cells or tissues. For example, algae, especially microalgae, are an abundant and inexpensive source of biomatter filler for biocomposites that has garnered increasing research attention in recent years [15–25]. Algae can be harvested in large quantities from aquatic cultures that do not occupy arable land or take up food production capacity [26]. In addition, the flexibility in their growth condition allows them to act as a reservoir for industrially-generated carbon by feeding on industrial emissions such as power station flue gas and providing biogenic carbon fixation [27,28].

One of the primary incentives for incorporating biomatter filler into commercially degradable polymers such as PLA is the enhanced biodegradability of the resulting biocomposites in natural environments. Previous studies showed that the incorporation of algae filler in PLA significantly increases the degradation rate of the resulting biocomposites under composting conditions as well as in soil at as low as 5 wt% algae concentration [17,29]. Similar improvements in soil degradation performance were also observed following the incorporation of *Ulva armoricana* and starch in a poly(vinyl alcohol) (PVA) matrix [18].

In terms of mechanical performances, many prior studies have reported an increase in material Young's modulus following the introduction of algal biomatter in different polymers. This stiffening is especially prevalent in intrinsically low-stiffness polymers such as poly (butylene succinate) (PBS), poly(butylene adipate-*co*-terephthalate) (PBAT) or PVA. For such polymers, Young's modulus enhancements ranging from 30% to above 100% have been reported for algal biomatter filler concentrations of 30 wt% [18–20]. The same phenomenon has also been reported for stiffer polymers to a lesser magnitude. Bulota et al. [21] reported a 25% increase in Young's modulus between their biocomposite with 40 wt% powderized green macroalgae filler and neat PLA. On the other hand, most studies have shown that the incorporation of algal biomatter leads to significant reductions in strength and elongation to failure in different polymer matrices, which is the most common and significant drawback of algal biocomposites [18–25].

These negative effects on strength and elongation to failure have mainly been attributed to the incompatibility between the biomatter filler and the polymer matrices, resulting in poor filler-matrix adhesion, and the formation of voids around filler particles [18,21]. The most common approach taken to address this filler-matrix incompatibility is via the grafting of a compatibilizing agent, such as maleic anhydride (MA) onto the matrix polymer [15,18,22,24,30,31]. For spirulina-polymer composites specifically, studies have reported increases in composite Young's modulus [24], strength [24,31], and elongation at break [24,31] following the introduction of MA-grafted matrix polymer.

Alternatively, filler-matrix adhesion may be improved by disrupting the biomatter filler using a physical treatment. This treatment would enable the reduction of the filler particle size and allow for higher total surface area at equal filler concentration, which in turn would induce higher degrees of filler-matrix interaction. The disruption and dissociation of biomatter cell walls also releases intracellular content that may allow for more favorable interactions between the biomatter filler and the polymer matrix [32]. Some benefits of physical over chemical treatments include the lifted requirement for additives, and the effective treatment of the entire biomatter, as compared to partial reaction between the matrix polymer and the chemical compatibilizer, bypassing issues of inhomogeneous distribution of the chemically modified phases. A number of different cell disruption techniques have been studied comparatively for their effectiveness on different microalgae species for applications such as lipid and protein extraction [33,34].

Here, we investigate sonication as a strategy to induce cell disruption as a strengthening process in PLA-spirulina biocomposites. Sonication provides numerous advantages such as short extraction time, high effectiveness and the ability to be carried out in benign solvents (such as water) on relatively small amount of samples [34–36]. As an example, Jantasrirad et al. [37] recently showed that the use of sonicated brown algae filler in a starch biopolymer matrix at 10 wt% filler concentration led to 330% and 230% improvements in the strength compared to neat starch biopolymer and the equivalent biocomposite with non-sonicated filler respectively. In our case, we hypothesize that the disruption of spirulina cellular structure will improve the adhesion between the spirulina filler and the PLA matrix by increasing the filler surface area and that the resulting reduction in filler particle size will also lead to improved filler dispersion in the matrix. To test our hypothesis, we compare the micromorphology of our biocomposites made using either sonicated or non-sonicated spirulina biomatter at different filler concentrations along with their mechanical and thermal properties.

2. Experimental section

2.1. Materials and sample fabrication

Spirulina powder purchased from nuts.com (Cranford, NJ, USA) was either used as-received (samples labelled as non-sonicated, NS) or after physical pretreatment (samples labelled as sonicated and freeze-dried, SF). For the SF samples, as-received spirulina powder was mixed with water at a 1:10 weight ratio and sonicated in an ice bath for 20 min using a Fisher Scientific Model 505 probe sonicator (Thermo Fisher; Waltham, MA, USA) with a titanium tip of diameter 3.81 mm (0.25″). After sonication, the biomatter suspension was freeze-dried using a lyophilizer (Freezone 2.5 L; Labconco Corp., Kansas City, MO, USA) to remove all water content and obtain the final processed spirulina.

Total Corbion (Gorinchem, Netherlands) Luminy LX175 PLA pellets were first ground up in an Eberbach E3300 cutting mill (Van Buren Charter Township, MI, USA) with a size 20 mesh, ensuring a characteristic particle size under 850 μm. The spirulina powder (NS or SF) was then premixed with the PLA granules using a FlackTek SpeedMixer (FlackTek; Landrum, SC, USA) for 60 s at 1000 rpm at nominal PLA-spirulina ratios of 100:1, 100:5, 100:10 and 100:30 by weight, corresponding to 1, 4.8, 9.1 and 23.1 wt%. Next, the dry mixtures were fed into a Thermo Fisher Scientific Process 11 parallel twin-screw extruder (Thermo Fisher; Waltham, MA, USA) to be melt-mixed and extruded through a 2 mm circular die, at a constant temperature of 170 °C across all heating zones and 10 rpm screw speed. After extrusion, the resulting PLA-spirulina filaments were pressed using a TMAX-RT-24D hot press (TMAXCN, China) at 170 °C to produce biocomposite sheets. Neat PLA samples were fabricated as reference following the same steps and parameters as the biocomposites minus the pre-mixing.

2.2. Material characterizations

Rectangular tensile strips of nominal gauge area of 4×40 mm^2 were cut from the hot-pressed composite sheets of nominal thickness 0.127 mm. Tensile tests were conducted at a constant strain rate of 0.005 s^{-1} on a Shimadzu AGS-X mechanical test frame (Shimadzu Scientific Instruments; Columbia, MD, USA) equipped with a 5 kN load cell. Before testing, samples were preconditioned in a desiccation chamber for a minimum of 24 h. At least 10 samples of each formulation were tested. We also studied the effect of water incubation on the mechanical properties of our PLA-spirulina biocomposites by performing tensile tests on the composite samples after 24 h of immersion in deionized (DI) water.

Optical microscopy slides of the spirulina water suspension (both NS and SF) were prepared and examined under a Motic Panthera TEC-BF microscope (Motic; Hong Kong, China) in transmission mode. For scanning electron microscopy (SEM), samples were sputter-coated with 4 nm of platinum on an EM ACE600 sputter coater (Leica Microsystems

GmbH; Wetzlar, Germany) before being examined using an Apreo VP SEM (Thermo Fisher Scientific; Waltham, MA, USA) with an accelerating voltage of 2 kV and a current of 13 pA.

The thermal stability of our biocomposites was evaluated through thermogravimetric analysis (TGA) on a TGA 550 analyzer (TA Instruments; New Castle, DE, USA). Each sample was heated under a nitrogen flow of 25 mL/min, from room temperature to 900 °C at a constant rate of 10C/min. From the mass loss data, the onset of degradation (T_o) was defined as the temperature at which 5% of the mass is lost, and the peak degradation temperatures (T_p), is defined as the temperature at the maximum degradation rate (peak of the DTG curve, defined by the first derivative of mass loss over temperature).

X-ray diffraction (XRD) was performed on a D8 Advance (Bruker, Germany). The X-ray source was Cu Kα, providing a wavelength of 1.54184 Å and was operated at 40 V and 40 A. Pure PLA and biocomposite samples were hot-pressed to a nominal thickness of 0.254 mm and trimmed to a 25 mm×25 mm surface area.

Fourier-transform infrared spectroscopy (FTIR) was performed on a Nicolet iS10 FT-IR spectrometer (Thermo Fisher; Waltham, MA, USA) in attenuated total reflection (ATR) mode. The scanning region was set in the range 4000–350 cm^{-1} with a resolution of 4 cm^{-1} over 20 scans. The results were then normalized with respect to their maximum absorbance.

Contact angle tests were performed in ambient conditions using a Krüss Drop Shape Analyzer and the contact angle measurements were produced by its software, ADVANCE (KRÜSS Scientific; Germany), using the in-built high-resolution CCD camera. For each composition, five separate droplets of 4 ± 1 μL of DI water were placed on the sheets of neat PLA and biocomposites. The contact angle was then determined as the average angle between the horizontal baseline (sample surface) and the left and right tangent (ellipse fit) of the droplet edge.

3. Results and discussion

3.1. Effect of sonication on spirulina characteristics

Building on previous studies which reported successful disruption of the cellular structure in spirulina and other microalgae using probe sonication [34,38], we subjected the spirulina filler to a sonication process aiming to decrease the filler particle size. Optical microscopy images of the unprocessed, as-received (non-sonicated, NS) spirulina as well as the sonicated and freeze dried (SF) spirulina in respective aqueous suspensions are shown in Fig. 1a and b. Our imaging results indicate that 20 min of probe sonication was sufficient for breaking down the chain structure of the spirulina organism, as evidenced by the absence of long chains in our microscopy images of the SF spirulina. We also confirm that cell wall rupture and cell dissociation (cell lysis) were achieved after sonication, as mostly subcellular fragments (instead of intact cells or organelles) were visible after sonication.

FTIR analysis of spirulina filler in both NS and SF form (see Fig. S1) reveals no differences in the chemical composition as a result of the treatment. In both cases, the fillers have strong absorption in the hydroxyl group stretch region at 3200–3300 cm^{-1}, C═O and C—O groups from carboxylic acids (C═O stretching peak at 1740 cm^{-1}, C—O stretching peak at 1040 cm^{-1}), and the most predominant, protein-related groups appear in both spectra (amide I band at 1600–1660 cm^{-1}, amide II at 1540 cm^{-1}, and amide III vibrations in 1230–1240 cm^{-1}) [16,39]. Both spectra also show the carbohydrate-related bands with multiple peaks including C—H stretching at 2800–2900 cm^{-1}, CH_3, CH_2, and C—H bending at 1380–1450 cm^{-1} from polysaccharides or lipids, and C—O stretching peaks at 1090 and 1160 cm^{-1} [16,39].

The SEM images of dry NS and SF spirulina powder presented in Fig. 1c and d, corroborate the chain disintegration and cell dissociation of spirulina observed under optical microscope following sonication and freeze-drying. As can be seen in Fig. 1d, SF spirulina takes the form of irregular small fragments and flakes, with no apparent cellular structure. Particle analysis based on the SEM images confirms successful filler size reduction as a result of the sonication process, with the characteristic particle size decreasing from 28.3 ± 16.6 μm to 5.5 ± 3.5 μm (see particle size distributions in Fig. S2a). The specific surface area (using ellipsoidal and flake-like approximation for the geometry of the NS and SF particles, respectively) increased after sonication from 0.3 ± 0.1 μm^{-1} to 3.1 ± 0.5 μm^{-1} (see Fig. S2b). We note that in the as-received form, spirulina chains are further agglomerated into clusters, resulting in a larger characteristic particle size than anticipated from optical microscopy observations.

This stark morphological difference of NS versus SF spirulina leads to clearly distinguishable visual appearances of their resulting biocomposites, as depicted in Fig. 1e-h. At macroscale, the SF PLA-spirulina biocomposites are more homogeneous than the NS biocomposites, with fewer visible spirulina aggregates at PLA-filler ratio below 100:10 (Fig. 1e, f). However, we observed large spirulina agglomerates in the SF

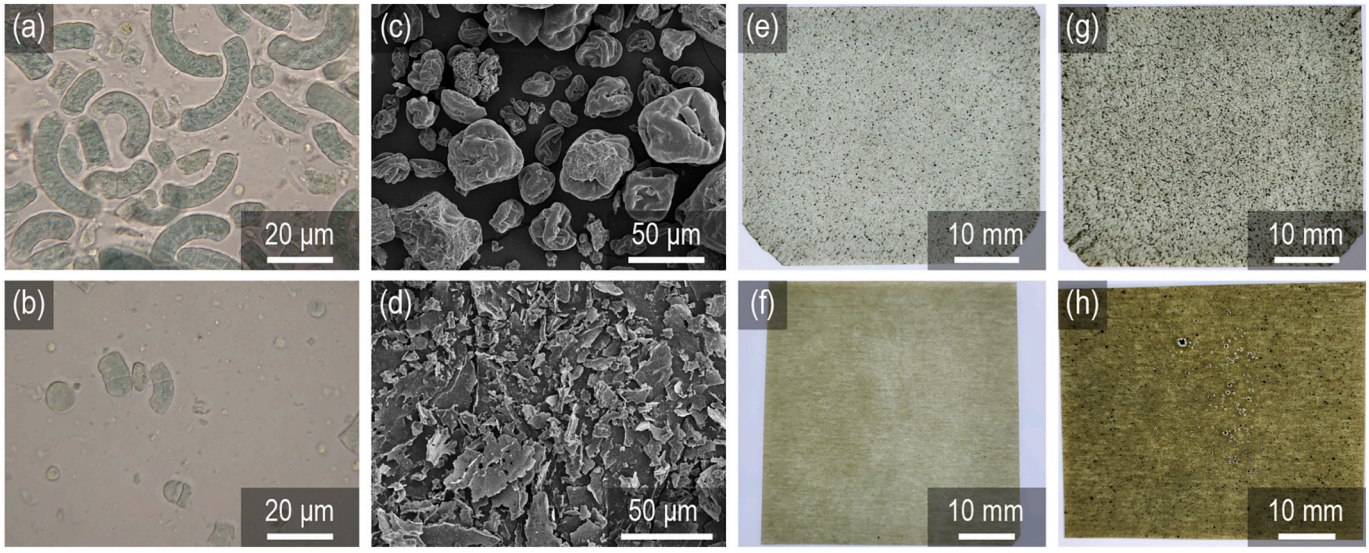

Fig. 1. Effect of preprocessing on the morphology of spirulina powder and the resulting biocomposites. Optical microscopy images of NS (a) and SF (b) spirulina in suspension; SEM images of NS (c) and SF (d) spirulina powder (dry); Photographs of biocomposite samples NS 100:10 (e), SF 100:10 (f), NS 100:30 (g), and SF 100:30 (h).

biocomposites at 100:30 ratio (hundreds of microns in scale) that are significantly greater in size than those at 100:10 ratio (Fig. 1f, h). In contrast, we did not see a substantial increase in aggregate size in NS biocomposites resulted from increase in filler concentration from 100:10 to 100:30 (Fig. 1e, g).

3.2. Composite mechanical properties and morphology

In Fig. 2a, we show representative stress-strain curves for neat PLA, SF, and NS biocomposites at all the tested filler concentrations. The measured values of the macroscopic Young's modulus (E), ultimate tensile strength (UTS), strain to failure (ε_{max}) and toughness are reported for these concentrations in Fig. 2c-f. Starting from the elastic response of the two sets of biocomposites, the results show that the incorporation of any amount of spirulina irrespective of the pretreatment, does not lead to significant changes in the Young's modulus of the biocomposites. As can be seen in Fig. 2c, the macroscopic Young's moduli in both NS and SF biocomposites do not vary significantly with respect to spirulina concentration. All biocomposites have an average macroscopic Young's modulus within ±13% of the PLA modulus (average of 2.30 GPa). The SF biocomposites showed statistically significant (p-value < 0.05) increases in E over NS biocomposites at 100:10 and 100:30 ratios, while a slight reduction in E was observed at the minimum tested filler ratio of 100:1.

In both NS and SF biocomposites, a decreasing trend in ultimate tensile strength (UTS) with increasing spirulina concentration was observed (Fig. 2d) starting at filler ratio of 100:5. This decrease is in agreement with prior literature which reported similar reductions in strength when chlorella or spirulina powder was introduced in other strong thermoplastic matrices [24,25] or when other types of algae were incorporated in PLA [21]. Still, our tensile tests revealed that at filler ratios higher than 100:5, the SF biocomposites had consistently higher UTS compared to the NS biocomposites. The relative magnitude of this difference increased from 7.9% at 100:5 filler ratio to 24.9% at 100:30 ratio. These results confirm our hypothesis that physical treatment of the filler can substantially improve the strength of the resulting biocomposites.

Indeed, the strength enhancement conferred to the biocomposites upon introduction of physically pretreated spirulina is only observed in our experiments at filler ratios above 100:5. In the 100:1 samples, the benefits from the improved filler dispersion and reduced filler size are not evident. At this concentration, the SF composite is slightly weaker than its NS counterpart. We hypothesize that at low filler concentrations, the large interface area of the well-dispersed SF powder induces more weakening than the sparsely distributed NS aggregates. Beyond the 100:5 ratio, the smaller size and improved dispersion of the SF filler begin to outweigh the benefits from having fewer inclusions in the NS case, resulting in the consistent strength deficit in the NS composites compared to their SF counterparts.

In terms of strain to failure (ε_{max}) and toughness, a similar decreasing trend was observed with increasing spirulina concentration (Fig. 2e, f). In both NS and SF biocomposites, the reductions in ε_{max} and toughness are approximately 60% and 80%, respectively, at the 100:30 filler ratio, consistent in order of magnitude with prior literature [24,25,29]. From our ε_{max} and toughness measurements, there is no statistically significant difference between SF and NS biocomposites in all but the 100:5 filler ratio. At 100:5 filler ratio, the SF biocomposite is 13% and 21.7% higher in ε_{max} and toughness respectively compared to the equivalent NS biocomposite. Additionally, we observe a moderate degree of post-elastic plasticity in neat PLA as well as some of the biocomposites with up to 100:5 filler ratio (Fig. S3). However, as we increase the concentration of spirulina in the biocomposites, we observe a progressive reduction in the degree of plasticity, and a clear transition in post peak behavior towards brittle failure. The results suggest that the increase of spirulina concentration in our biocomposites hinders energy dissipation mechanisms such as the re-orientation and sliding of the polymer chain which leads to reduced plastic deformation prior to failure and consequently lower ε_{max}.

We conducted XRD tests to identify if the presence of filler in any state influences the crystallinity of PLA (under the same processing conditions). The results, presented in Fig. 2b, show little difference between the diffraction patterns of neat PLA and those of the biocomposites, regardless of filler processing conditions, even at the maximum tested PLA-filler ratio of 100:30. For additional comparison, the XRD curves of as-manufactured (AM) PLA and post-annealed (cold crystallized, CC) PLA are presented in Fig. S4, showing the purely amorphous structure of PLA resulting from our manufacturing method that does not include any annealing steps. The consistency in sample crystallinity (or the absence there-of) between biocomposites and neat PLA samples suggests that the incorporation of spirulina filler did not change the amorphous structure of the PLA, and any differences in mechanical properties between them are unlikely rooted in the change in crystallinity of the PLA matrix. Therefore, the strength improvements observed in the SF biocomposites over the NS biocomposites are more likely induced by the change in filler properties or filler-matrix interactions as a result of the sonication and freeze-drying, rather than from change in matrix crystallinity.

SEM images of the biocomposite fracture surfaces (Fig. 3c, e) reveal

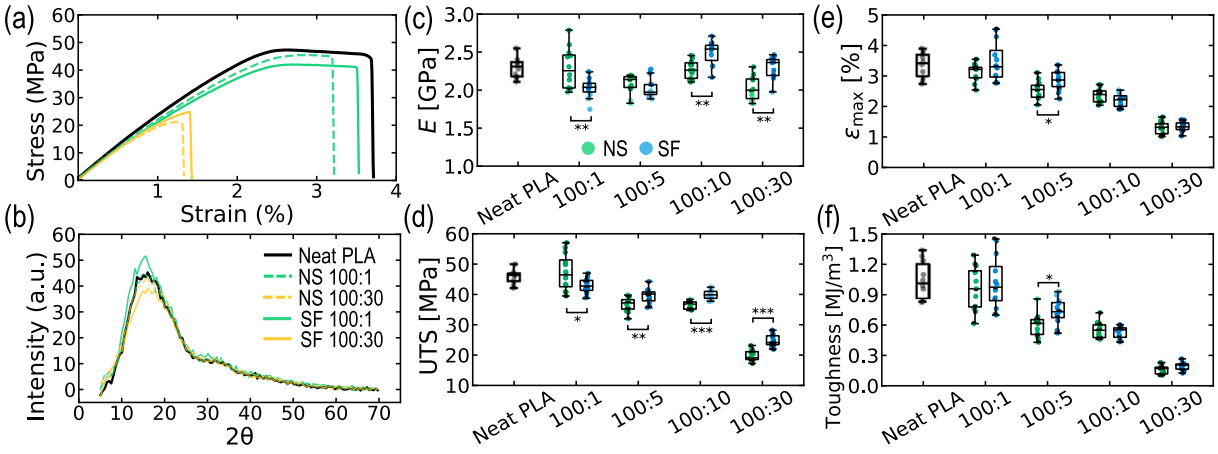

Fig. 2. Mechanical properties of the PLA-spirulina biocomposites. Representative stress-strain curves (a) and XRD patterns (b) of NS and SF PLA-spirulina biocomposites in selected concentrations; Young's modulus (c), Ultimate Tensile Strength (d), Strain to failure (e) and Toughness (f) of NS and SF PLA-spirulina biocomposites in all concentrations. The asterisks represent the level of statistical significance according to the Welch's t-test [40]. *$p < 0.05$, * * $p < 0.01$, and * * * $p < 0.001$.

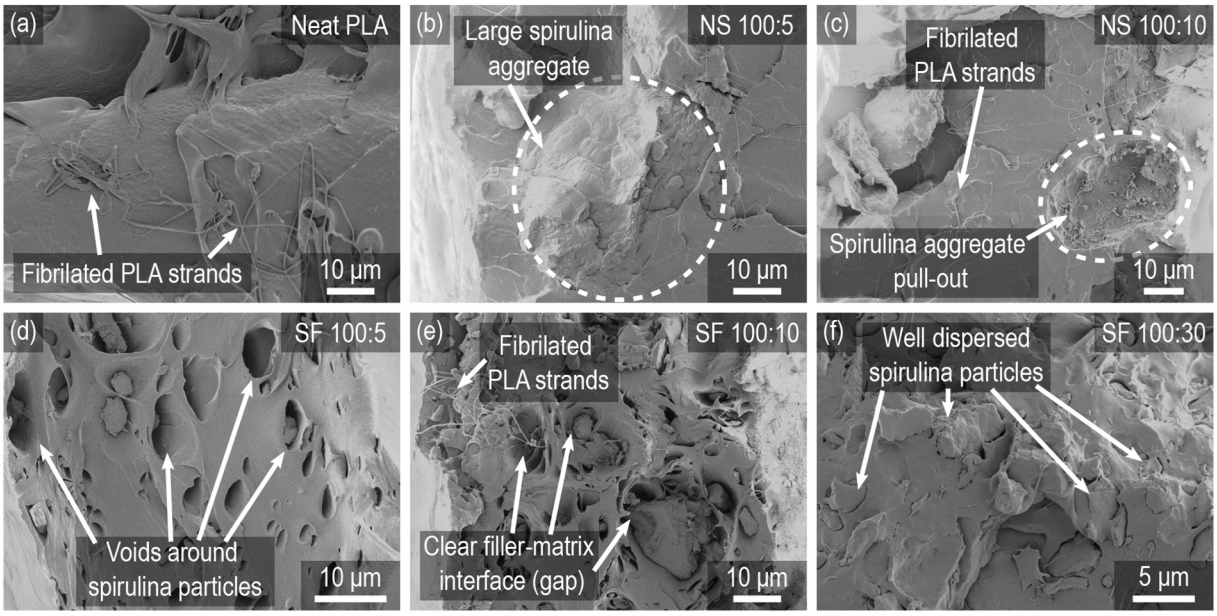

Fig. 3. SEM snapshots of the fracture surface of the biocomposites. Fracture surface of neat PLA (a), embedded large spirulina particle in NS sample (imprint of intact spirulina cellular structure) (b), site of large spirulina aggregate pull-out in NS sample (c), matrix deformation around spirulina particles forming larger pores and showing poor filler-matrix interface in SF sample (d), large range of spirulina particle size and poor filler matrix interface in SF sample (e), numerous and well-dispersed small spirulina particles in SF sample (f).

signs of local plasticity in the form of fibrillated polymer strands in the matrix-rich regions of our biocomposites. These features are consistent in form with those exhibited on the fracture surface of neat PLA from our own results (Fig. 3a) and are corroborated by results shown in prior literature [41]. Moreover, the SEM images corroborated our visual observations of improved homogeneity in the SF biocomposites, as we remarked reduced particle size and improved distribution of spirulina filler in the SF biocomposites compared to the NS biocomposites. It is evident that the reduction in spirulina particle size and changes in particle morphology induced by sonication and freeze-drying (previously observed in powders before melt-compounding, Fig. 1d) are largely retained in the SF biocomposites, and likely led to the improved distribution of the filler as shown in Fig. 3d-f.

Similarly, the particle morphology of the NS spirulina was also retained throughout the composite manufacturing process, as can be seen in Fig. 3b and c. Although large agglomerates of spirulina filler (hundreds of microns in particle size) were observed at the macroscale in the SF 100:30 samples (Fig. 1h), they occur sparingly and are spaced far apart. In these samples, we still observed distinct and well-dispersed spirulina fragments as the dominant type of filler morphology at the microscale, as shown in Fig. 3f, for example. Therefore at filler ratio above 100:10, we observed two dominant types of filler morphology in the SF biocomposites: well-dispersed cell fragments with minimum aggregation (10 to 50 μm in particle size) at the microscale, and larger macroscopic clusters of unincorporated spirulina biomatter.

In addition, SEM results revealed poor bonding between spirulina and PLA in both NS and SF biocomposites at all studied concentrations. The clear separation at the matrix-filler interface upon fracture indicates the lack of adhesion and incompatibility between the two components. In the NS 100:10 example shown in Fig. 3c, a crater is observed to be left behind from the pull-out of a large spirulina aggregate. This lack of compatibility was not aided by the filler pretreatment, as evident by the voids formed around spirulina particles in Fig. 3d and the clear filler-matrix gap and matrix deformation around spirulina particles in Fig. 3e.

FTIR analysis of the biocomposites (Fig. S5) revealed that their spectra is dominated by the absorption peaks of PLA, as anticipated. Specifically, in the neat PLA sample and in all the biocomposites the peaks at 3000 and 2960 cm^{-1} associated with C—H stretching in CH_3, the 1752 cm^{-1} attributed to C═O stretch, the 1460 and 1366 cm^{-1} of C—H bending in CH_3, and finally the C-O-C stretching vibrations with peaks at 1190 and 1087 cm^{-1} [42,43] are all present. Spirulina, even at the highest concentration, shows only a minimal contribution at 1650 cm^{-1} (amide I peak from proteins) in the spectra of the biocomposites. The lack of differences in the peak positions and intensities when comparing the spectra of the biocomposites with NS and SF corroborates our hypothesis from SEM observations that there poor bonding between the filler and PLA is not improved or affected by the sonication treatment, as no new bond formation or otherwise changes were detected from the FTIR analysis.

Based on our results from FTIR and morphological analysis, we conclude that sonication and freeze-drying of spirulina allows for a particle size reduction, surface area increase and better filler dispersion, but does not improve the adhesion or bonding between the filler and the PLA matrix. Therefore, we propose that the reduced filler size and improved filler dispersion facilitated the strength enhancements in SF biocomposites compared to NS biocomposites at filler ratios above 100:5.

3.3. *Effects of water exposure on the composite mechanical properties*

Due to the generally hydrophilic nature of biopolymers, the effects of humidity on their mechanical properties is significant and well studied [44,45]. For example, the presence of water below a certain threshold in cellulose facilitates a plasticization effect by enabling improved chain sliding, which ultimately toughens cellulose [45]. However, above a critical threshold, the presence of water has detrimental effects in cellulose, as it disrupts the chain rearrangement mechanisms and load transfer during deformation, thereby leading to weakening and loss of toughness.

On the other hand, PLA undergoes minimal changes in mechanical properties in response to water exposure below the threshold that facilitates hydrolysis reactions [46]. Therefore, we hypothesize that water exposure can be used to induce plasticization on the spirulina filler while having minimal effect on the matrix, which can lead to improved toughness in the resulting biocomposites.

To characterize the effect of humidity on our composites (with and

without pretreatment to spirulina filler) we performed water contact angle tests in our biocomposites, and mechanically tested our samples after immersion in water for 24 h. The mean contact angles of neat PLA and biocomposites are plotted and compared in Fig. S6. Mechanical test results for neat PLA controls and biocomposites at filler ratios of 100:10 and 100:30 are reported in Fig. 4 and Fig. S7. The moisture contents of each mechanically tested biocomposite configuration after 24 h water immersion are tabulated in table S3.

All the biocomposites showed similar water contact angles, slightly lower than pure PLA, with the SF composites having marginally lower values than their NS counterparts across different filler concentrations. We did not observe any clear trends in contact angle measurements with respect to increasing filler content in either NS or SF biocomposites.

On the other hand, the mechanical tests reveal noteworthy differences in our biocomposites. We observe that the Young's modulus (Fig. 4b) is mostly unaffected after water immersion in neat PLA and NS 100:10 biocomposite, while the SF 100:10 biocomposite showed a moderate drop in E of 14.1% after water immersion. The moduli underwent more significant drops in the 100:30 biocomposite. On average, E decreased by 38% for the NS and by 33% for the SF samples, showing that the biocomposites with pretreated filler favorably maintain a slightly higher Young's modulus compared their counterpart with untreated filler. This loss of stiffness at higher spirulina concentrations could be attributed to the water-induced softening of the spirulina inclusions.

The strain to failure (Fig. S7) increased drastically in the water-immersed SF biocomposite at 100:10 filler ratio (64.5% increase, compared to the same material tested dry). The NS 100:10 samples, on the other hand, showed only a moderate increase in ε_{max} of ~10.6%, resulting in a 38.7% difference in ε_{max} between the SF and NS biocomposites following water immersion. At 100:30 filler ratio, ε_{max} increased by 34% and 44% for the NS and SF biocomposites respectively following water immersion, confirming the larger enhancement effects on ε_{max} from water immersion in the SF biocomposites.

We measured moderate reductions in tensile strength of 13.0% and 12.6% respectively for the NS and SF biocomposite with 100:30 filler ratio following water immersion (Fig. 4c). In contrast, the biocomposite at 100:10 filler ratio showed no significant change in strength following water immersion for either filler processing conditions.

Finally, in terms of toughness (Fig. 4d), we observed significant increases at 18%, 94%, and 42% for NS 100:10, SF 100:10 and SF 100:30 samples respectively following water immersion. The change in toughness for the NS 100:30 samples was statistically insignificant. The difference in toughness between the SF and the NS samples at 100:10 filler ratio increased from statistically equal to 58% following water immersion. We can see from the stress-strain curves shown in Fig. 4a and Fig. S3 that the large increases in ε_{max} and toughness seen in the SF 100:10 sample following water immersion can be attributed to its substantial increase in post-peak plasticity, a change that is less prevalent in the other sample configurations tested.

The lack of any significant change in measured mechanical behavior of our dried versus water-immersed neat PLA samples suggests that changes related to the filler must be the primary contributor behind the significant shift in mechanical properties observed in our biocomposites. From the contact angle measurements and moisture absorption measurements, we can see that the difference in hydrophilicity and the ability to uptake water are not affected by filler processing, suggesting that the difference in mechanical performances between NS and SF biocomposites following water immersion are unlikely to have resulted from different level of water uptake.

Therefore, we hypothesize that the plasticization effect of water in our PLA-spirulina biocomposites is predominantly caused by the water-induced softening of the spirulina clusters via diffusion within the PLA matrix, which is enhanced by the improved filler distribution resulting from the mechanical pretreatment to our spirulina filler. As detailed in previous sections, the distribution of the spirulina filler was more homogeneous in the SF 100:10 than in the SF 100:30 samples, in which we observed the emergence of larger spirulina aggregates. In turn, the better filler distribution of the SF 100:10 samples was reflected in the large increase in ε_{max} in the water-immersed samples.

3.4. Composite thermal properties

We assessed the thermal stability of our materials through TGA measurements presented in Fig. 5a (SF) and Fig. S8a (NS). From these results, the onset degradation temperatures (T_o) and peak degradation temperatures (T_p) of NS and SF biocomposites were obtained and tabulated in Table 1. Neat PLA reaches a 5% mass loss at 328.8 °C, and has a maximum degradation rate (DTG peak) at 367.8 °C, in agreement with prior literature [47]. The addition of spirulina (either NS or SF) consistently and progressively reduces the T_o and T_p of resulting biocomposites with increasing filler content, indicating a decrease in

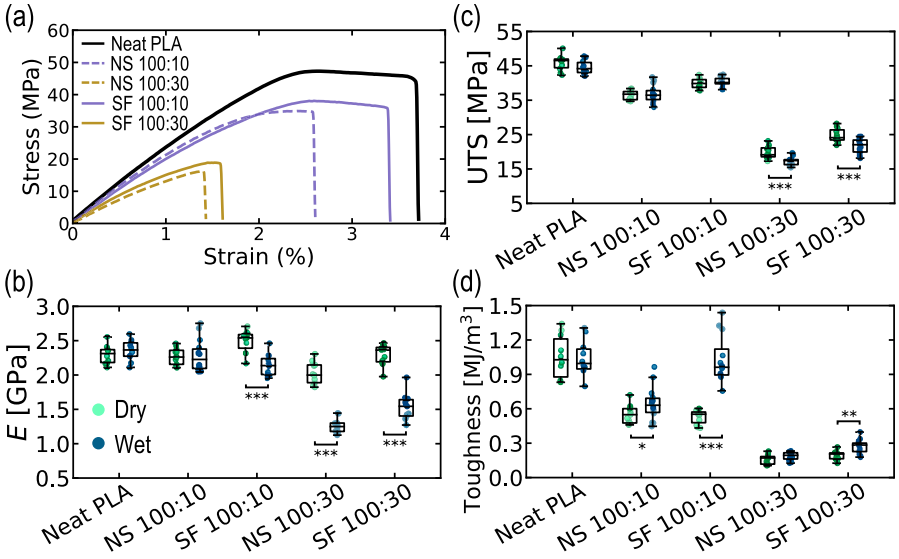

Fig. 4. Mechanical properties of the PLA-spirulina biocomposites following 24 h water immersion. Young's modulus (a), Tensile strength (b), and Strain to failure (c) of dry and wet PLA-spirulina biocomposites in all tested configurations.

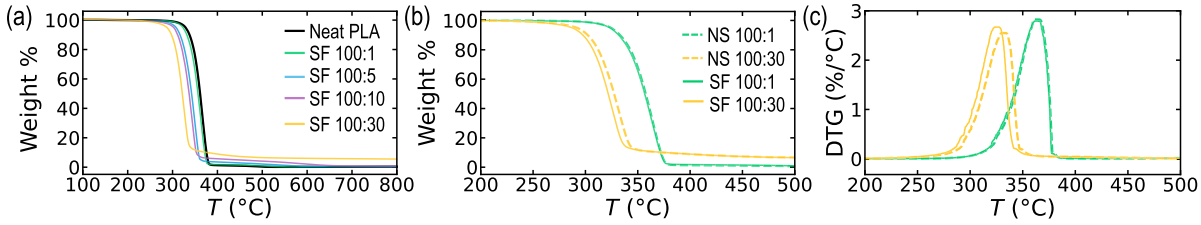

Fig. 5. TGA curves of SF PLA-spirulina biocomposites of all concentrations (a); TGA (b) and DTG (c) curves of SF and NS PLA-spirulina biocomposites in 100:1 and 100:30 concentrations.

Table 1
Onset degradation temperatures (5% mass loss), T_o; Peak degradation temperatures (DTG peak), T_p.

PLA-Spirulina Ratio	T_o^{NS} (°C)	T_o^{SF} (°C)	T_p^{NS} (°C)	T_p^{SF} (°C)
Neat PLA	328.8		367.8	
100:1	324.2	323.2	363.8	363.5
100:5	310.5	307.7	356.5	351.3
100:10	304.6	302.4	347.0	345.1
100:30	291.8	287.3	332.8	325.9

thermal stability as a result of biomatter loading. These results were anticipated from the lower thermal stability of pure spirulina compared to PLA (see Fig. S10 and table S4).

The pretreatment of spirulina cells led to small yet detectable differences in the thermal properties of the produced biocomposites. The graphs in Fig. 5b and c highlight the processing effects on the biocomposites with highest and lowest filler contents. At the 100:1 PLA-filler ratio, there is no difference in the mass loss profiles of NS and SF biocomposites, while at the 100:30 ratio a small shift to lower temperatures is observed for the SF biocomposites compared to the NS, indicating a reduction in thermal stability as a result of the processing of biomatter filler. Overall, the SF biocomposites had T_o values between 1 and 4.5C lower than the corresponding NS biocomposites, and T_p values between 1.9 and 6.9 °C lower, with greater differences for biocomposites with higher spirulina concentration.

The TGA data also reveal a clear increasing trend in residual weights at 500 °C with increasing spirulina loading in both NS and SF biocomposites. These residual weight percentages at 500 °C are 0.7(0.9), 1.9(2.2), 3.4(4.1), 6.6(6.5) for 100:1, 100:5, 100:10, and 100:30 NS(SF) ratios respectively. Such differences are anticipated as neat PLA degrades completely during pyrolysis leaving zero residue, while the pyrolysis result of spirulina powder shows a non-zero char yield (see Fig. S10a). However, these differences in residual weight amongst biocomposites with filler concentration up to 100:10 diminish after ~600 °C, as we observe a secondary mass loss event that leads to indistinguishable differences between their final residual weights. The only exceptions are the 100:30 samples (both NS and SF), which retained significantly higher residues compared to other groups at the end of the heating cycle. This finding suggests that, the char formed by biocomposite at 100:30 spirulina concentration is more stable than the char formed by biocomposites at lower spirulina concentrations at 600 °C, in agreement with prior literature [19,20].

3.5. Environmental assessment

To provide a measure of the effects of our biocomposites in the green house gas (GHG) emissions, we focused on the global warming potential (GWP) on a conventional 100-year timescale using values from published studies. The GWP associated with PLA production is dependent on the source of feedstock as well as manufacturing methods. They are well studied and documented for popular commercial PLA products [48,49]. From values published in 2019, the GWP of the Corbion PLA from growth of feedstock to factory door is +0.501 kg CO_2 eq per kg of PLA [49].

Concerning our biomatter filler, the GHG emissions and GWP from the production of spirulina biomatter (as well as other microalgae) is strongly dependent on its cultivation method and processing conditions. CO_2 emissions associated with operating parameters of microalgae cultivation such as pumping, heating, growth media composition (e.g., fertilizers), and artificial light intensity (if used) can vary drastically depending on the combination of conditions chosen in each particular case [27,50–54]. Upon growth, spirulina has been reported to uptake 1.72 to 1.8 kg of CO_2 for each kg (dry mass) of spirulina produced [50,51]. It has also been shown that the CO_2 required for microalgae cultivation can be supplied in the form of power plant flue gas, thereby allowing carbon uptake from algae growth to be regarded as biogenic carbon sequestration and hence calculated as a negative value in GWP evaluations [27,28].

Combining GWP values for the cultivation and manufacturing of spirulina (39% dry weight) [50] with the energy consumption of drying microalgae [27], we estimate the total GWP for dry spirulina powder manufactured using renewable energy to be approximately −0.54 kg CO_2 eq/kg of dry spirulina. The resulting GWP reductions from incorporating spirulina biomatter in PLA biocomposites at the tested concentrations are summarized in Table 2.

4. Conclusions

In this work, we reported the morphological, mechanical and thermal properties of PLA-spirulina biocomposites and specifically explored the effect of using physically dissociated filler through sonication as a mean for performance enhancement. Mechanical testing revealed that the elastic properties of PLA were retained in the biocomposites at matrix:filler ratios as high as 100:30. The use of mechanically dissociated spirulina filler over its unprocessed counterpart led to notable tensile strength improvements in the resulting biocomposites at filler ratios higher than 100:5, owing to reduced filler particle size, higher surface area and improved filler distribution. We also showed that the use of dissociated filler allows significant toughening of the PLA-spirulina biocomposite after immersion in water via water-induced filler plasticization. Notably, at 100:10 filler ratio, the SF samples achieved a 58% higher average toughness than the NS samples, even rivaling the toughness of neat PLA. Taking into account the carbon-negative growth of microalgae, our environmental analysis showed that the incorporation of spirulina biomatter filler is effective at reducing the global warming potential of a carbon-positive polymer such as PLA.

Table 2
Global Warming Potential (GWP) reduction from spirulina biomatter incorporation

PLA-Spirulina Ratio	GWP Reduction (%)
100:1	2.10
100:5	10.0
100:10	18.9
100:30	47.9

Future work could explore the effect of physical filler pretreatment in the crystallization behavior of PLA, and study how the biomatter filler at different states influences the biodegradation mechanisms in the biocomposites. It is also worth studying the potential synergistic effects of physical filler dissociation in conjunction with other forms of filler/matrix pretreatments, such as chemical matrix compatibilization and/or filler pre-plasticization. Processing conditions such as pressing and extrusion temperature as well as extrusion speed can be further explored and optimized for larger scale applications and potential property improvements.

CRediT authorship contribution statement

Kuotian Liao: Methodology, Software, Validation, Formal analysis, Investigation, Data curation, Writing – original draft, Visualization. **Paul Grandgeorge:** Conceptualization, Data curation, Software, Formal analysis, Visualization, Writing – review & editing. **Andrew M. Jimenez:** Formal analysis, Conceptualization, Software, Investigation, Writing – original draft. **Bichlien H. Nguyen:** Conceptualization, Supervision. **Eleftheria Roumeli:** Writing – review & editing, Formal analysis, Conceptualization, Supervision, Resources, Funding acquisition.

Declaration of Competing Interest

The authors declare that they have no known competing financial interests or personal relationships that could have appeared to influence the work reported in this paper.

Data availability

Data will be made available on request.

Acknowledgments

The authors thank Kate M. McGrath-Flinn, Ian Campbell, Mallory Parker, Hareesh Iyer, and Jeremy L. Fredricks for assisting in the preparation of the sonicated and freeze-dried spirulina, biocomposites fabrication, contact angle, FTIR, and TGA analysis. K.L. acknowledges funding from the University of Washington (College of Engineering Dean's Fellowship). The authors acknowledge financial support in the form of gift funds from Microsoft Research.

Appendix A. Supplementary data

Supplementary data to this article can be found online at https://doi.org/10.1016/j.susmat.2023.e00591.

References

[1] R. Geyer, J.R. Jambeck, K.L. Law, Production, use, and fate of all plastics ever made, Sci. Adv. 3 (2017), e1700782.
[2] D.K. Schneiderman, M.A. Hillmyer, 50th anniversary perspective: there is a great future in sustainable polymers, Macromolecules 50 (2017) 3733–3749.
[3] A.Z. Naser, I. Deiab, B.M. Darras, Poly (lactic acid)(PLA) and polyhydroxyalkanoates (PHAs), green alternatives to petroleum-based plastics: a review, RSC Adv. 11 (2021) 17151–17196.
[4] T. Jiang, Q. Duan, J. Zhu, H. Liu, L. Yu, Starch-based biodegradable materials: challenges and opportunities, Adv. Ind. Eng. Polym. Res. 3 (2020) 8–18.
[5] Z. Li, J. Yang, X.J. Loh, Polyhydroxyalkanoates: opening doors for a sustainable future, NPG Asia Mater. 8 (2016) e265.
[6] A. Arias, G. Feijoo, M.T. Moreira, Technological feasibility and environmental assess- ment of polylactic acid-nisin-based active packaging, Sustain. Mater. Technol. 33 (2022), e00460.
[7] K. Litauszki, D. Gere, T. Czigány, Á. Kmetty, Environmentally friendly packaging foams: investigation of the compostability of poly (lactic acid)-based syntactic foams, Sustain. Mater. Technol. 35 (2022), e00527.
[8] K. Liao, Experimental and Numerical Investigation of the Mechanical Behavior and Morphological Characteristics of 3D Printed Materials Made Via Fused Deposition Mod- Eling (FDM), M.Sc. thesis,, University of Washington, 2021.
[9] A.A. Singh, M.E. Genovese, G. Mancini, L. Marini, A. Athanassiou, Green processing route for polylactic acid–cellulose fiber biocomposites, ACS Sustain. Chem. Eng. 8 (2020) 4128–4136.
[10] M.E. Genovese, L. Puccinelli, G. Mancini, R. Carzino, L. Goldoni, V. Castelvetro, A. Athanassiou, Rapid solvent-free microcrystalline cellulose melt functionalization with l-Lactide for the fabrication of green poly (lactic acid) biocomposites, ACS Sus- tain. Chem. Eng. 10 (2022) 9401–9410.
[11] V. Nagarajan, A.K. Mohanty, M. Misra, Perspective on polylactic acid (PLA) based sustainable materials for durable applications: focus on toughness and heat resistance, ACS Sustain. Chem. Eng. 4 (2016) 2899–2916.
[12] F. Ansari, M. Salajkova, Q. Zhou, L.A. Berglund, Strong surface treatment effects on reinforcement efficiency in biocomposites based on cellulose nanocrystals in poly (vinyl acetate) matrix, Biomacromolecules 16 (2015) 3916–3924.
[13] J. Shojaeiarani, D.S. Bajwa, N.M. Stark, T.M. Bergholz, A.L. Kraft, Spin coating method improved the performance characteristics of films obtained from poly (lactic acid) and cellulose nanocrystals, Sustain. Mater. Technol. 26 (2020), e00212.
[14] J. Song, C. Chen, S. Zhu, M. Zhu, J. Dai, U. Ray, Y. Li, Y. Kuang, Y. Li, N. Quispe, et al., Processing bulk natural wood into a high-performance structural material, Nature 554 (2018) 224–228.
[15] S. Onen Cinar, Z.K. Chong, M.A. Kucuker, N. Wieczorek, U. Cengiz, K. Kuchta, Bioplastic production from microalgae: a review, Int. J. Environ. Res. Public Health 17 (2020) 3842.
[16] J.L. Fredricks, H. Iyer, R. McDonald, J. Hsu, A.M. Jimenez, E. Roumeli, Spirulina-based composites for 3D-printing, J. Polym. Sci. 59 (2021) 2878–2894.
[17] N.K. Kalita, N.A. Damare, D. Hazarika, P. Bhagabati, A. Kalamdhad, V. Katiyar, Biodegradation and characterization study of compostable PLA bioplastic containing algae biomass as potential degradation accelerator, Environ. Challeng. 3 (2021), 100067.
[18] E. Chiellini, P. Cinelli, V.I. Ilieva, M. Martera, Biodegradable thermoplastic composites based on polyvinyl alcohol and algae, Biomacromolecules 9 (2008) 1007–1013.
[19] C. Toro, M.M. Reddy, R. Navia, M. Rivas, M. Misra, A.K. Mohanty, Characterization and application in biocomposites of residual microalgal biomass generated in third generation biodiesel, J. Polym. Environ. 21 (2013) 944–951.
[20] S. Torres, R. Navia, R. Campbell Murdy, P. Cooke, M. Misra, A.K. Mohanty, Green composites from residual microalgae biomass and poly (butylene adipate-co-terephthalate): processing and plasticization, ACS Sustain. Chem. & Eng. 3 (2015) 614–624.
[21] M. Bulota, T. Budtova, PLA/algae composites: morphology and mechanical properties, Compos. A: Appl. Sci. Manuf. 73 (2015) 109–115.
[22] T. Otsuki, F. Zhang, H. Kabeya, T. Hirotsu, Synthesis and tensile properties of a novel composite of Chlorella and polyethylene, J. Appl. Polym. Sci. 92 (2004) 812–816.
[23] M.M. Hassan, M. Mueller, M.H. Wagners, Exploratory study on seaweed as novel filler in polypropylene composite, J. Appl. Polym. Sci. 109 (2008) 1242–1247.
[24] N. Zhu, M. Ye, D. Shi, M. Chen, Reactive compatibilization of biodegradable poly (butylene succinate)/Spirulina microalgae composites, Macromol. Res. 25 (2017) 165–171.
[25] M.A. Zeller, R. Hunt, A. Jones, S. Sharma, Bioplastics and their thermoplastic blends from Spirulina and Chlorella microalgae, J. Appl. Polym. Sci. 130 (2013) 3263–3275.
[26] J.C. Pires, COP21: the algae opportunity? Renew. Sust. Energ. Rev. 79 (2017) 867–877.
[27] B.D. Beckstrom, M.H. Wilson, M. Crocker, J.C. Quinn, Bioplastic feedstock production from microalgae with fuel co-products: a techno-economic and life cycle impact assessment, Algal Res. 46 (2020), 101769.
[28] J.H. Duarte, E.G. de Morais, E.M. Radmann, J.A.V. Costa, Biological CO2 mitigation from coal power plant by Chlorella fusca and Spirulina sp, Bioresour. Technol. 234 (2017) 472–475.
[29] M. Simonič, F.L. Zemljič, Production of bioplastic material from algal biomass, Chem. Ind. Chem. Eng. Quart. 27 (2021) 79–84.
[30] K. Wang, Bio-Plastic Potential of spirulina Microalgae, M.Sc. thesis,, University of Geor- gia, 2014.
[31] Dianursanti, C. Noviasari, L. Windiani, M. Gozan, Effect of compatibilizer addition in Spirulina platensis based bioplastic production, in: AIP Conference Proceedings, 2019, p. 030012.
[32] A.P. Larrosa, A.S. Camara, J.M. Moura, L.A. Pinto, Spirulina sp. biomass dried/disrupted by different methods and their application in biofilms production, Food Sci. Biotechnol. 27 (2018) 1659–1665.
[33] K.-Y. Show, D.-J. Lee, J.-H. Tay, T.-M. Lee, J.-S. Chang, Microalgal drying and cell disruption–recent advances, Bioresour. Technol. 184 (2015) 258–266.
[34] P. Prabakaran, A.D. Ravindran, A comparative study on effective cell disruption methods for lipid extraction from microalgae, Lett. Appl. Microbiol. 53 (2011) 150–154.
[35] R. Halim, T.W. Rupasinghe, D.L. Tull, P.A. Webley, Mechanical cell disruption for lipid extraction from microalgal biomass, Bioresour. Technol. 140 (2013) 53–63.
[36] M. Kurokawa, P.M. King, X. Wu, E.M. Joyce, T.J. Mason, K. Yamamoto, Effect of sonication frequency on the disruption of algae, Ultrason. Sonochem. 31 (2016) 157–162.
[37] S. Jantasrirad, J. Mayakun, A. Numnuam, K. Kaewtatip, Effect of filler and sonication time on the performance of brown alga (Sargassum plagiophyllum) filled cassava starch biocomposites, Algal Res. 56 (2021), 102321.
[38] S. Dey, V.K. Rathod, Ultrasound assisted extraction of β-carotene from Spirulina platensis, Ultrason. Sonochem. 20 (2013) 271–276.
[39] Á. Barón-Sola, M. Toledo-Basantes, M. Arana-Gandía, F. Martínez, C. Ortega-Villasante, T. Dučić, I. Yousef, L.E. Hernández, Synchrotron radiation-Fourier

transformed infrared microspectroscopy (μSR-FTIR) reveals multiple metabolism al- terations in microalgae induced by cadmium and mercury, J. Hazard. Ma- ter. 419 (2021), 126502.
[40] B.L. Welch, The generalization of 'STUDENT'S' problem when several different popu- lation varlances are involved, Biometrika 34 (1947) 28–35.
[41] S.-D. Park, M. Todo, K. Arakawa, Effect of annealing on the fracture toughness of poly (lactic acid), J. Mater. Sci. 39 (2004) 1113–1116.
[42] B.W. Chieng, N.A. Ibrahim, W.M.Z. Wan Yunus, M.Z. Hussein, Poly(lactic acid)/ poly (ethylene glycol) polymer nanocomposites: effects of graphene nanoplatelets, Polymers 6 (2013) 93–104.
[43] H.L.C. Pulgarin, C. Caicedo, E.F. López, Effect of surfactant content on rheological, thermal, morphological and surface properties of thermoplastic starch (TPS) and polylactic acid (PLA) blends, Heliyon 8 (2022), e10833.
[44] A.J. Benítez, J. Torres-Rendon, M. Poutanen, A. Walther, Humidity and multi- scale structure govern mechanical properties and deformation modes in films of native cellulose nanofibrils, Biomacromolecules 14 (2013) 4497–4506.
[45] Y. Hou, Q.-F. Guan, J. Xia, Z.-C. Ling, Z. He, Z.-M. Han, H.-B. Yang, P. Gu, Y. Zhu, S.-H. Yu, et al., Strengthening and toughening hierarchical nanocellulose via humidity-mediated interface, ACS Nano 15 (2020) 1310–1320.
[46] M. Niaounakis, E. Kontou, M. Xanthis, Effects of aging on the thermomechanical properties of poly(lactic acid), J. Appl. Polym. Sci. 119 (2011) 472–481.
[47] F. Carrasco, P. Pagès, J. Gámez-Pérez, O. Santana, M.L. Maspoch, Processing of poly (lactic acid): characterization of chemical structure, thermal stability and mechanical properties, Polym. Degrad. Stab. 95 (2010) 116–125.
[48] E.T. Vink, S. Davies, Life cycle inventory and impact assessment data for 2014 IngeoTM polylactide production, Ind. Biotechnol. 11 (2015) 167–180.
[49] A. Morão, F. De Bie, Life cycle impact assessment of polylactic acid (PLA) produced from sugarcane in Thailand, J. Polym. Environ. 27 (2019) 2523–2539.
[50] A. Tzachor, A. Smidt-Jensen, A. Ramel, M. Geirsdóttir, Environmental impacts of large-scale Spirulina (Arthrospira platensis) production in Hellisheidi geothermal park Iceland: life cycle assessment, Mar. Biotechnol. 24 (2022) 991–1001.
[51] R. Rodríguez, J. Espada, J. Moreno, G. Vicente, L. Bautista, V. Morales, A. Sánchez-Bayo, J. Dufour, Environmental analysis of Spirulina cultivation and biogas production using experimental and simulation approach, Renew. Energy 129 (2018) 724–732.
[52] S. Papadaki, K. Kyriakopoulou, M. Stramarkou, I. Tzovenis, M. Krokida, Environmental assessment of industrially applied drying technologies for the treatment of Spirulina platensis, IOSR J. Environ. Sci. Toxicol. Food Technol. 11 (2017) 41–46.
[53] C. Ye, D. Mu, N. Horowitz, Z. Xue, J. Chen, M. Xue, Y. Zhou, M. Klutts, W. Zhou, Life cycle assessment of industrial scale production of spirulina tablets, Algal Res. 34 (2018) 154–163.
[54] S. Smetana, M. Sandmann, S. Rohn, D. Pleissner, V. Heinz, Autotrophic and heterotrophic microalgae and cyanobacteria cultivation for food and feed: life cycle assess- ment, Bioresour. Technol. 245 (2017) 162–170.